Time-varying vibration characteristics and surface topography of thin-walled cylinders during machining operations

Kaibo Lu[1*], Xun Chen[2], Fengbin Liu[1], Fengshou Gu[3]

1. College of Mechanical and Vehicle Engineering, Taiyuan University of Technology, Shanxi 030024, China

2. School of Engineering, Liverpool John Moores University, Liverpool L3 3AF, UK

3. School of Computing and Engineering, University of Huddersfield, Huddersfield HD1 3DH, UK

* Corresponding author. Email: lvkaibo4@163.com; Tel: +86-139-0341-8795

Abstract

Machining thin-walled cylindrical workpieces is prone to vibration due to their weak stiffness, leading to complicated surface topography. Knowledge of the dynamic behaviors of the thin-walled structures during machining plays a fundamental role in the production quality control for real life applications. This paper presents the variation of the vibration characteristics of thin-walled cylinder turning as well as its effect on the machined surface topography due to the removal of materials. The influences of variable wall thicknesses and cutting positions on the vibration characteristics of the workpiece are analyzed. It is shown that the circumferential shell vibrational mode is more sensitive to the variation of the tube thickness than the axial beam mode. The response of the tube to the dynamic cutting force under each vibrational mode varies along the cutting path. The stability limits of the machining process become decreased as the cutting tool moves toward the free end of the workpiece. In the machining trials of thin-walled tubes, it was found that the features of the vibration frequency as well as machined surface texture of the thin-walled cylinders are shifting in a cutting pass. The physical mechanism behind this phenomenon could be interpreted according to dynamics and kinematics of machining. By extracting the critical vibration frequency and surface waviness along the cutting path, a data-driven surface topography was reconstructed, which showed consistency with the real machined surface topography. The formulated correlation between the vibration characteristics and the surface topography provides a holistic understanding of dynamic behaviors of thin-walled cylinder machining, and a tool that utilizes vibration to produce functional microstructures.

Key words: Thin-walled cylinders; Machining; Chatter mode shift; Surface topography reconstruction.

1. Introduction

Thin-walled cylindrical components are widely used in aerospace and automotive industry, which are prone to vibration under operating conditions due to their low rigidity and damping [1-4]. Analysis of a thin-wall turning operation can be considered in two different scenarios, including the vibration of a thin-walled cylinder as an element assembled in an engineering system [5-11], and as a workpiece manufactured

on machine tools [12-21]. The knowledge of dynamic behaviors of a thin-walled structure is therefore of great practical importance for machining performance evaluation and production quality control in industrial applications.

As cases of the former scenario, Zhang et al. [5] and Li [6] analyzed the free vibration characteristics of thin cylindrical shells with various boundary conditions including clamped-clamped, clamped-free, and simply supported-simply supported using wave propagation approaches. Rawat et al. [7] calculated the modal frequencies of the cylindrical shells using the finite element method and compared the results with analytical solutions. In these papers, the shells under investigation were all assumed to be at rest. Considering the effects of centrifugal and Coriolis forces as well as initial hoop tension due to rotation, Li and Lam [8], Sun et al. [9] studied the effect of boundary conditions on the frequency characteristics of a thin rotating cylindrical shell through the generalized differential quadrature method and Fourier series expansion method, respectively. In recent years, many scholars have been focused on the vibration problems of rotating cylindrical shells coupled with composite materials or structures [10,11]. Overall, there have been a number of investigations that were aimed at vibration analysis of thin-walled parts affiliated to engineering systems. In this case, the structural dimensions and dynamics remained unchanged in operation, and thus the modal parameters of the parts are time-invariant.

In the latter scenario, however, the vibration analysis could be more complicated due to the changing dynamics of thin-walled workpieces caused by the removal of materials during machining processes, which corresponds to a time-variant vibrating system. Chatter vibrations, one of the major limitations in machining processes, result from the interaction between the cutting process and the machine tool structure [12-14]. The chatter vibration phenomenon of thin-walled cylindrical tubes in turning processes was first reported by Arnold [15] in 1961. In his study, the author interpreted the cause of the lobe-shaped chatter patterns formed on the surface according to the mode of vibration of the machined part. Chang and Lai [16,17] pointed out that the machining chatter occurrence of thin wall tubes is mainly dependent on the workpiece diameter to the wall thickness (D/H) ratio, and the stiffness of the shell mode is decreased significantly with the D/H ratio increased. Mehdi et al. [18-20] presented theoretical and experimental studies on dynamics of thin-walled tubular parts under various cutting conditions. The effect of damping on machining stability was emphasized, whereas the influence of the varying dynamic characteristics of the machined part was not considered. Lorong et al. [21] introduced a time-domain simulation method for modeling dynamics of a thin-walled part in turning operations. The influence of cutting speed and damping on chatter stability was analyzed. Considering the effect of the varying workpiece dynamics, Fischer et al. [22] proposed a parametric model for stability prediction of an internal turning operation. Through numerical simulation the tool feed rate was optimized to improve the production efficiency. Gerasimenko et al. [23,24] conducted investigations into chatter behaviors in turning of thin-walled tubular workpieces by combining analytical modeling and experimental measurements. The effect of the variable compliance of the workpiece on process stability was also discussed.

A great number of efforts have been made on the vibration analysis of thin-walled structures. However, the dynamic behavior as well as its effect on the surface topography creation during thin-walled cylindrical turning has rarely been investigated systematically. It is known that the rotating workpiece in a turning operation is cut as the tool is traveling along the axis of the workpiece. As a result, the dynamics of the workpiece vary due to the removal of materials. By comparison with solid structures, the dynamic characteristics of thin-walled structures seem to be more sensitive to the material removal in cutting processes [17,18,25]. In addition, the conditions under which chatter instability occurs vary with the cutting positions [12-14]. The moving tool-workpiece contact point is thus to induce a position-dependent response to the cutting force generated during machining.

In this paper, the correlation between the vibration characteristics and the surface topography of thin-walled cylinders in turning process has been identified, which contributes to a holistic understanding of the thin-walled cylinder machining. Based on the numerical model of thin-walled workpieces under machining conditions, the influence of the variable wall thickness and cutting position on the vibration characteristics is analyzed theoretically. After that, experimental modal measurements and machining trials of the thin-walled cylindrical tubes were carried out to verify the theoretical analysis. The time-varying vibration features along the cutting path were extracted and used for the surface topography reconstruction. Finally, discussions and conclusions are given.

2. Dynamic model of a rotating cylindrical shell

Considering that the rigidity of the thin-walled cylindrical workpiece is usually far less than that of the cutting tool or machine tool structures, the workpiece is often regarded as the only compliant body in the machining system. The clamped-free boundary condition, that is, the workpiece is clamped by a chuck at one end and free at the other end, which is widely used for internal or external turning process in real-life applications, is considered in this study.

The reference surface of the cylindrical shell is taken at the middle surface where a cylindrical coordinate system (x,θ,z) is fixed. The coordinates of x , θ and z are respectively taken in the axial, circumferential and radial directions of the shell, as shown in Fig. 1(a). The shell under investigation is with length L, radius R, and thickness H and rotates around its axis at an angular velocity N. The tool moves along the axis of the workpiece with the feed rate f. The displacements of the shell are defined by u , v and w in the x , θ and z directions, respectively. The thin wall cylindrical workpiece vibrates in combination of the beam mode and the shell mode. Its modal shapes are shown in Fig. 1(b).

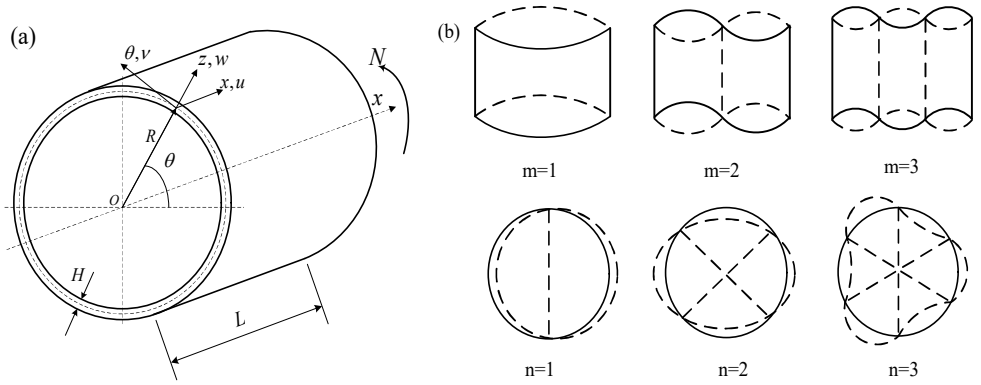

Fig. 1 A rotating cylindrical shell (a) and its mode shapes (b)

Based on the Kirchhoff-Love shell theory, the governing differential equations of the rotating thin-walled cylinder are formulated using the Hamilton's principle [26]

$$\begin{aligned}
&\frac{\partial N_x}{\partial x}+\frac{1}{R}\frac{\partial N_{x\theta}}{\partial \theta}+N_\theta^0\left(\frac{1}{R^2}\frac{\partial^2 u}{\partial \theta^2}-\frac{1}{R}\frac{\partial w}{\partial x}\right)=\rho H\frac{\partial^2 u}{\partial t^2}\\
&\frac{1}{R}\frac{\partial N_\theta}{\partial \theta}+\frac{\partial N_{x\theta}}{\partial x}+\frac{Q_\theta}{R}+\frac{N_\theta^0}{R}\frac{\partial^2 u}{\partial x\partial \theta}=\rho H\frac{\partial^2 v}{\partial t^2}+2\rho HN\frac{\partial w}{\partial t}-\rho HN^2 v\\
&\frac{\partial Q_x}{\partial x}+\frac{\partial Q_\theta}{R\partial \theta}-\frac{N_\theta}{R}+\frac{N_\theta^0}{R^2}\left(\frac{\partial^2 w}{\partial \theta^2}-\frac{\partial v}{\partial \theta}\right)=\rho H\frac{\partial^2 w}{\partial t^2}-2\rho HN\frac{\partial v}{\partial t}-\rho HN^2 w
\end{aligned} \tag{1}$$

where $N_\theta^0=\rho HN^2R^2$ is the initial tangential stress generated by the centrifugal force due to rotation, where ρ is the density of the shell material; $\rho H\frac{\partial^2 u}{\partial t^2}$, $\rho H\frac{\partial^2 v}{\partial t^2}$ and $\rho H\frac{\partial^2 w}{\partial t^2}$ are the inertial forces; $2\rho HN\frac{\partial w}{\partial t}$ and $2\rho HN\frac{\partial v}{\partial t}$ are the Coriolis forces; $\rho HN^2 v$ and $\rho HN^2 w$ are centrifugal forces; Q_x and Q_θ are the transverse shear forces per unit length along the mid-plane in the x and θ directions, respectively.

The governing differential equations of the rotating thin-walled cylinder can be rearranged and written in matrix form as

$$\begin{pmatrix} L_{11} & L_{12} & L_{13}\\ L_{21} & L_{22} & L_{23}\\ L_{31} & L_{32} & L_{33}\end{pmatrix}\begin{pmatrix} u\\ v\\ w\end{pmatrix}=0 \tag{2}$$

where L_{ij} (i,j=1,2,3) are the partial differential operators with respect to x and θ. For free vibration of the thin cylindrical shell, according to the mode superposition method the displacements can be expressed as

$$\begin{cases} u(x,\theta,t) = \sum_{m=1}^{\infty}\sum_{n=1}^{\infty} U\phi_m^u(x)\cos(n\theta+\omega_{mn}t) \\ v(x,\theta,t) = \sum_{m=1}^{\infty}\sum_{n=1}^{\infty} V\phi_m^v(x)\sin(n\theta+\omega_{mn}t) \\ w(x,\theta,t) = \sum_{m=1}^{\infty}\sum_{n=1}^{\infty} W\phi_m^w(x)\cos(n\theta+\omega_{mn}t) \end{cases} \tag{3}$$

where U, V, and W are the displacement amplitudes in the x, θ and z directions, respectively; $\phi_m^k(x)$ (k=u,v,w) are the axial modal functions describing the mode shape of the shell in the longitudinal direction; ω_{mn} is the natural frequency corresponding to the vibration mode (m, n) of the workpiece, where m denotes the axial half-wave number and n denotes the circumferential wave number as seen in Fig. 1. By substituting the displacement functions into Eq. (2), the characteristic equation of the natural frequency of the rotating shell can be obtained as

$$\omega_{mn}^6 + \omega_{mn}^4\beta_1 + \omega_{mn}^3\beta_2 + \omega_{mn}^2\beta_3 + \omega_{mn}\beta_4 + \beta_5 = 0 \tag{4}$$

where β_i (i=1,2..5) are constants which can be found from the boundary conditions of the workpiece. Clearly, the vibration of the compliant workpiece at any given cutting position directly affects the machined surface texture. According to the kinematics of machining [27], the surface topography determined by the relative motion between the tool and the workpiece can be predicted in the cylindrical coordinate by

$$\begin{cases} x_c(t) = Nft/2\pi \\ \theta_c(t) = Nt \\ z_c(t) = w(x_c,\theta_c,t) \end{cases} \tag{5}$$

where x_c, θ_c and z_c are the coordinates of the cutting point. It is evident that the closed-form solutions of the dynamic system may become intractable as a result of the time-varying dimension of the workpiece in machining operations. For this reason, a numerical simulation is used for the vibration analysis of the machined thin-walled circular workpiece in this present study.

3. Numerical analysis of variable vibration characteristics of the thin-walled cylinder machining

When a thin-walled cylindrical workpiece is being machined, the thickness of the cylinder as well as the point on the cylinder surface where the cutting force is acting changes. This section deals with the influence of the variable wall thicknesses and cutting points on the vibration characteristics of the machined thin-walled cylinder with numerical approach.

Given the fact that the spindle-chuck assembly has a non-negligible effect on dynamics of compliant parts [18,28,29], the finite element model for the numerical simulation is constructed in terms of an industrial machine tool which is the same as the one used for the subsequent machining experiments. The detailed modeling procedure can be found in our previous study [29]. The benchmark thin-walled cylindrical workpiece under investigation has the length L=195 mm, the inner radius R=111 mm, and the wall thickness H=1.5 mm. The material of the workpiece is with the Young modulus E = 206000 MPa and density ρ = 7860kg/m^3. One end of the workpiece is clamped by a chuck and the other end is free. Fig. 2 presents the first three vibration modes of the thin-walled cylindrical workpiece with the clamped-free fixture fashion.

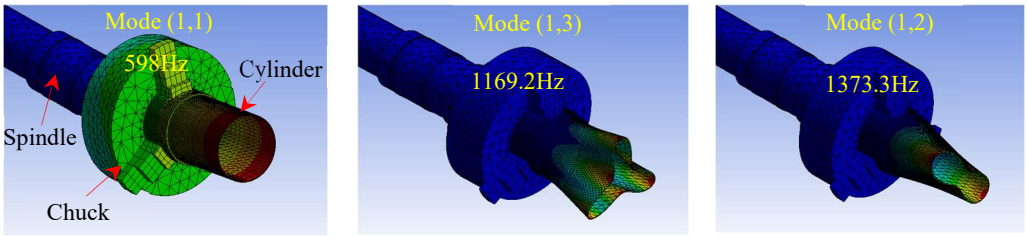

Fig. 2 The first three mode shapes of the thin-walled cylinder by numerical analysis

3.1 Effect of wall thickness on modes of vibration of the shell workpiece

After a cutting operation, the thickness of the thin-walled cylindrical workpiece is decreased due to the removal of material from the surface of workpiece. As the geometry changes, the vibration characteristics of the workpiece also vary accordingly. Since the low-order modes of vibration contribute mainly to dynamic response of a

mechanical system, the influence of the thickness variation on the first five vibration modes of the thin-walled cylinder under the clamped-free end condition is analyzed, as shown in Fig. 3.

It can be seen that except that the first-order bending mode does not change significantly, the natural frequencies of other modes descend evidently with the thickness decreased. The corresponding mode shapes change as well. Furthermore, in the first three modes the circumferential wave number of the shell shifts between 1 and 4, whereas the axial half-wave number remains unchanged. It indicates that the circumferential shell mode is more sensitive to the variation of the wall thickness of the workpiece. In addition, the vibration mode of the shell in the circumferential direction becomes more complex as the wall thickness gets thinner.

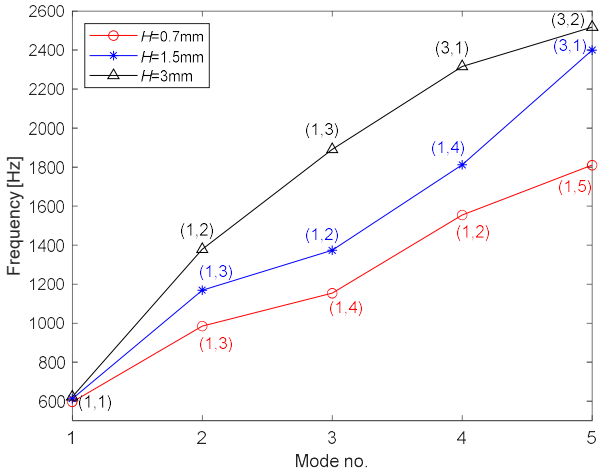

Fig. 3 Effect of the wall thickness on vibration modes of the thin-walled cylinder

3.2 Effect of cutting positions on frequency response functions

During a turning operation the cutting position of the tool varies along the workpiece axis in real time. Thus, the point where the cutting force is acting on the workpiece changes continuously as well. Fig. 4 provides comparison of the frequency response function (FRF) of the clamped-free shell at different cutting locations originated from the chuck end. It is shown that the vibration response of the thin cylinder obviously differs along the cutting path, demonstrating the non-uniform distribution of dynamic characteristics of the workpiece along its axis. The farther away from the chuck end, the greater the vibration response.

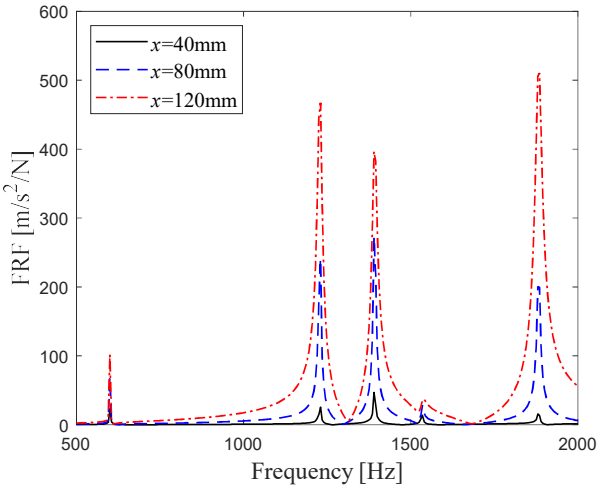

Fig.4 Effect of moving tool positions on dynamic response of the thin-walled cylinder

Technically, the cylindrical workpiece being turned resembles a stepped tube with time-varying dimensions during operation, as shown in Fig. 5(a). The variation of vibration modes of the tube along the cutting path is presented in Fig. 5(b), wherein the depth of cut *d* is assumed 0.8 mm. It is seen that the natural frequency corresponding to the beam mode (1,1) of the workpiece keeps nearly unchanged, but the frequencies corresponding to the shell modes generally exhibit a downward trend except the mode (1,2). Therefore, it can be inferred that the dominant vibration mode of the workpiece could differ at various cutting positions. Near the chuck end of the shell, the mode of the axial bending vibration dominates, whereas the mode of the circumferential shell vibration dominates near the free end. Correspondingly, the surface topography, determined mainly by the relative motion between the workpiece and the tool at the contact point, could also differ along the cutting path.

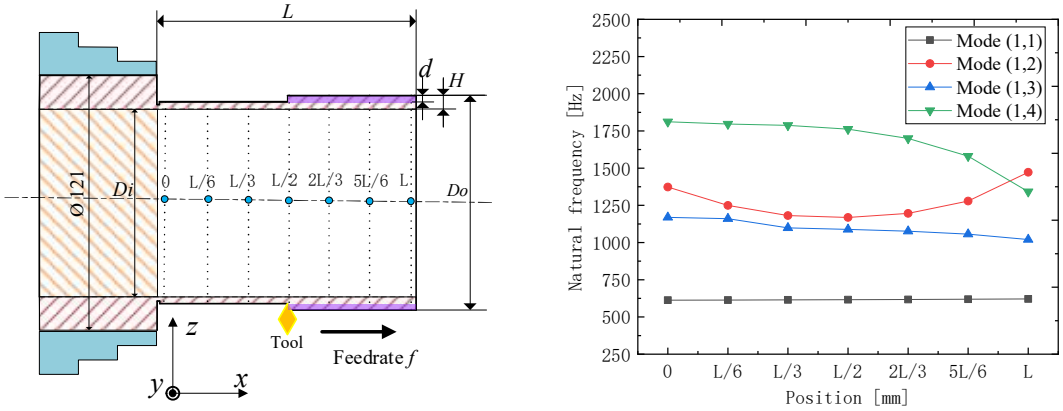

Fig. 5 Schematic diagram of the tube in turning (a) and variation of vibration modes of the tube along the cutting path (b).

4. Experimentation and discussion

4.1 Experimental setup

To verify the prior theoretical analysis and investigate the effect of the vibrational behavior on surface texture of thin-walled tubes in turning, the impact hammer tests and machining trials were carried out on a CA6140 conventional horizontal lathe with the maximum available power of 7.5 kW. The experimental setup is shown in Fig. 6.

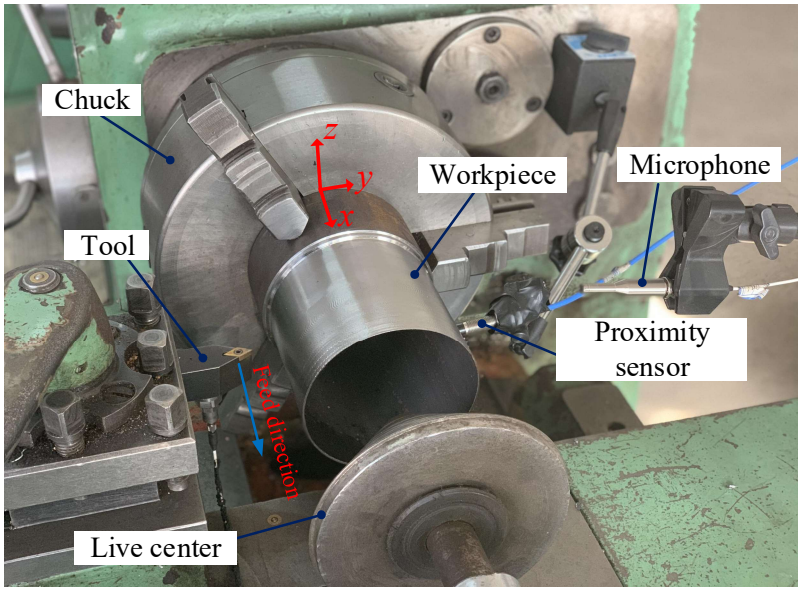

Fig. 6 Experimental setup

Table 1 Designed parameters for the turning experiments

Workpiece No.	Length L (mm)	Inner diameter D (mm)	Thickness H (mm)	Rotational speed Ω (rpm)	Depth of cut d (mm)	Feed rate f (mm/r)
Tube A	195	111	1.5	583	0.8	0.1
Tube B	160	111	1.5	583	0.8	0.1
Tube C	160	130	1.5	583	0.8	0.1

Three typical thin-walled cylindrical tubes were chosen and presented for comparison, in which Tube A had the same dimensions as the reference workpiece in the simulation section. The workpiece material is AISI 1040 steel. Before the machining tests, all the tubes with the initial wall thickness of 5 mm were cut off to be 1.5 mm thick with the support of a live center. The cutting tool DCMT11T304 carbide insert had the nose angle 55°, the nose radius 0.4 mm, and the clearance angle 7°, respectively. One fresh tool insert was utilized for each cutting test so as to reduce the effect of tool wear on the vibration response of the workpiece.

During the machining trials, one end of the tested tube was clamped by the three-jaw chuck and the other end was free without tailstock center support. The tool was fed along the $+x$ direction in turning tests. The designed machining parameters for the trials are summarized in Table 1. An eddy current sensor supported by a magnetic stand was used to acquire the displacement of the tube, and an omnidirectional acoustic sensor mounted near the machined tube was used for collecting the sound pressure generated during machining. A handheld data acquisition system, CoCo-80, was applied to collect the two signals synchronously with the sample rate of 10.24 kHz. After the machining, a portable roughness measuring instrument, MarSurf PS10, was used to obtain the surface roughness along the length of the workpiece.

4.2 Results and discussion

4.2.1 FRF measurements

For the hammer impact testing, an accelerometer was employed to acquire the response to the hammer excitation at the impact point on the tube at rest and then the frequency response function (FRF) of the machined tube was calculated. Fig. 7 depicts the comparison of the measured acceleration FRFs of the three test tubes at their midpoints. It can be readily obtained that decreasing the length-to-diameter ratio of the cylinder could stiffen the axial beam mode with the increased eigen-frequency; but increasing the D/H ratio could weaken the circumferential shell mode with the decreased eigen-frequency.

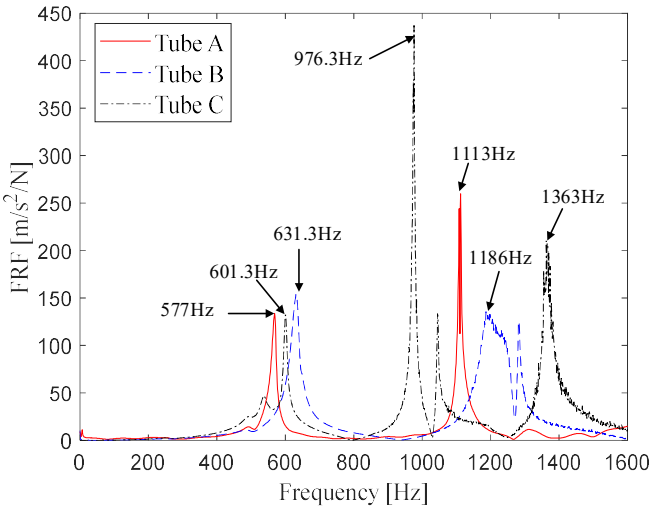

Fig. 7 Comparison the measured FRFs of the three test tubes

The effects of the varying wall thickness and cutting position on the measured FRF of the tube were investigated, as shown in Figs. 8 and 9. From Fig. 8, it can be seen that the vibration response of the tube was increased with the decrease of its wall thickness. Comparing the measured FRFs with the simulated vibration modes shown in Fig. 3 confirms that the circumferential shell mode of the hollow cylinder is more sensitive to the variation of the wall thickness than the axial beam mode.

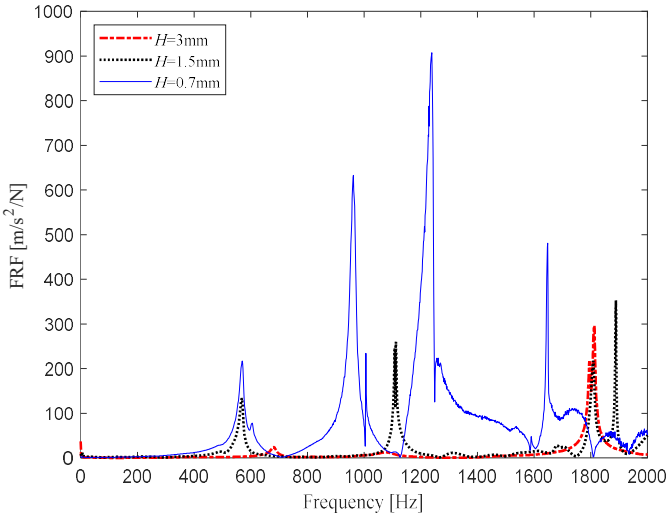

Fig. 8 Comparison of the measured FRFs of Tube A with different wall thickness

Fig. 9 illustrates the FRFs of the workpiece with the wall thickness 1.5 mm at three different positions along its axial direction. As the cutting position moved away from the chuck end, the vibration response of the thin-walled cylindrical workpiece generally strengthened. At a given cutting position, the amplitude at the frequency corresponding to each mode was different, indicating that the different mode shapes made different contributions to the system vibration. This shows consistency with the simulation results at the low frequency range as shown in Fig. 4. The reason for the frequency inconsistency at the high frequency range could be due to the geometric imperfections or boundary nonlinearities in the experimental model.

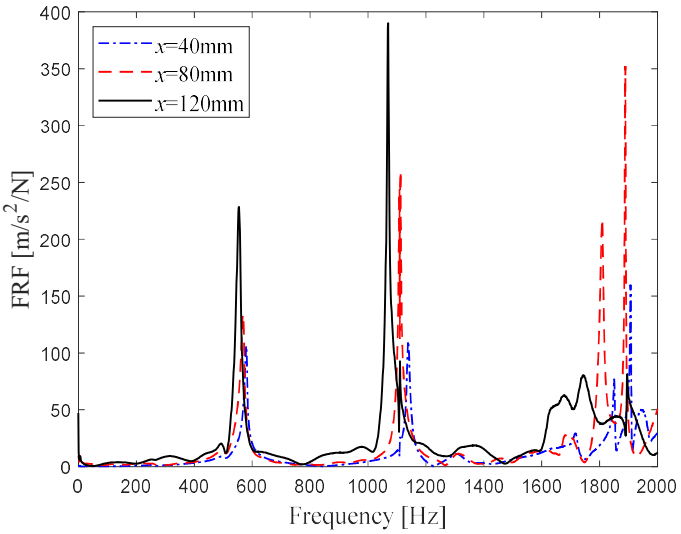

Fig. 9 Comparison of the measured FRFs of Tube A at different positions along its length

4.2.2 Signal features and surface topography

In the machining tests, the cutting tool moved along the workpiece from the chuck side to the free end. Initially, the cutting process was stable; when the tool arrived at a specific location, chatter began to occur and harsh noises surrounded in the field. It was interesting to note that the sound intensity went through the course of strengthening to weakening repeatedly when the machining instability continued to progress. As an example, Fig. 10 shows the sound and displacement signals during the machining process of Tube A. It can be seen that both the waveforms exhibited saw-toothed shapes in the late period of process.

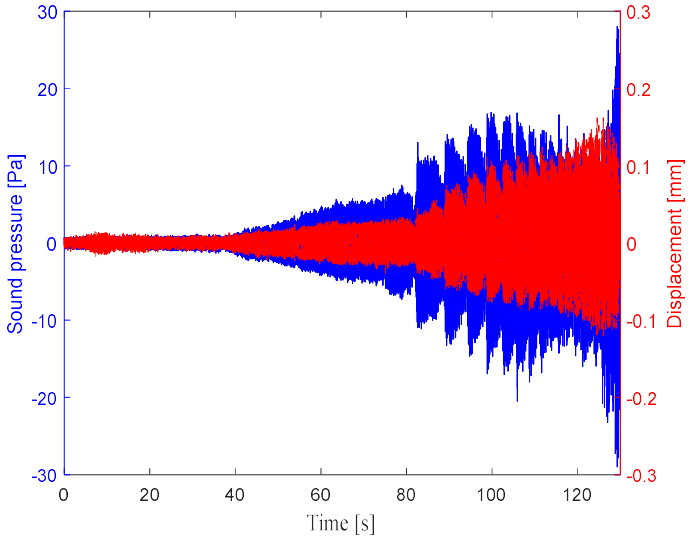

Fig. 10 Sound and displacement during turning of Tube A

The finished surface of Tube A after cutting is presented in Fig. 11. Interestingly, there were visibly distinctive regular chatter marks left on the machined surface. According to the appearance as well as the surface roughness of the marks, the tube surface was divided into three zones, including the stable zone, chatter zone 1 and chatter zone 2, respectively. These zones were characterized by the smooth surface, the spiral grooves and the lobe-shaped patterns, respectively. It is readily seen that the surface topography at zone 2 shows strong variability as the signal waveform does.

To fully understand the physical mechanism behind this phenomenon, first of all, the time-frequency analysis of the signals emitted by the turning process was conducted. Fig. 12 provides the spectra of the airborne acoustic signals for Tube A, wherein the components with the power less than -30 dB were filtered out to highlight the dominant frequency components. It is seen that when the machining process was stable, the vibration response was dominated by the rotation frequency component due to the eccentricity of the rotating workpiece or spindle. In the cutting interval 40 mm$<x<$78 mm corresponding to the chatter zone 1 shown in Fig. 11, the critical chatter frequency nearly remained f_{c1} =622 Hz. But in the interval 78 mm$<x<$130 mm corresponding to the chatter zone 2, the critical chatter frequency shifted to f_{c2} =1122 Hz accompanied by its harmonics and was decreased gradually as the tool approached the free end of the workpiece. Thus, it is reasonable to speculate upon the correlation between the formation of the special surface topography and the change of the dominant vibration frequency.

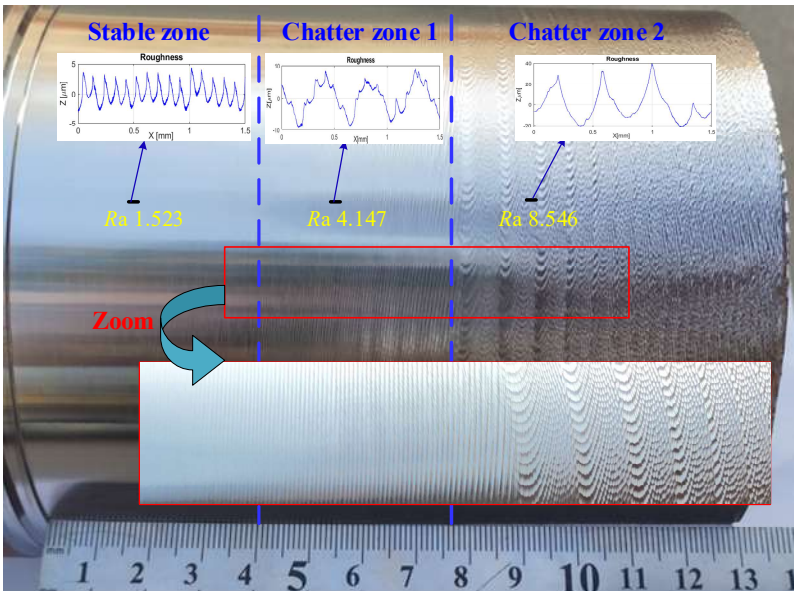

Fig. 11 Photo of the finished surface of Tube A after turning process

By extracting the critical vibration frequency and the amplitude of the roughness measurement along the cutting path and then using Eq. (5), the data-driven surface textures of Tube A can be reconstructed according to the kinematics of turning process, as shown in Fig. 13. The simulated textures resemble the real surface as shown in Fig.11, proving that the formation of the special surface patterns was mainly attributed to the variation of chatter characteristics. In essence, the spatial coherence, the phase difference of the adjacent textures on the cylindrical surface, resulted in different chatter patterns. When the chatter frequency remained constant, the phase between the two adjacent modulations formed by the oscillation trajectory of the compliant workpiece relative to the tip of the tool, was unchanging and the chatter patterns were regularly distributed. When the chatter frequency varied during turning, the phase difference would change accordingly, thus leaving complex footprints generated on the surface.

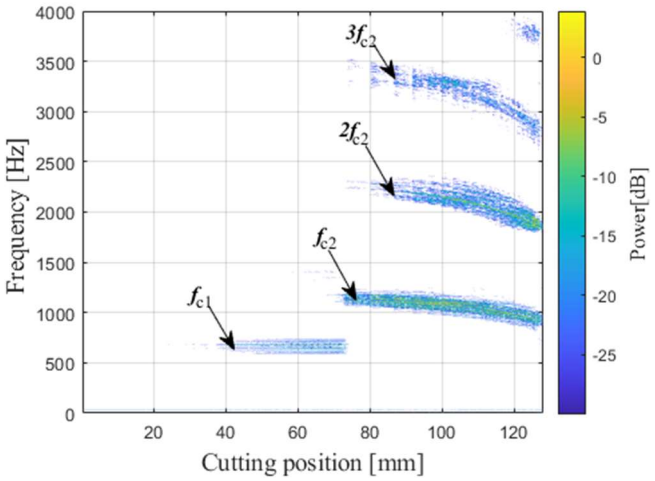

Fig. 12. Time-frequency analysis of the sound signals in turning of Tube A

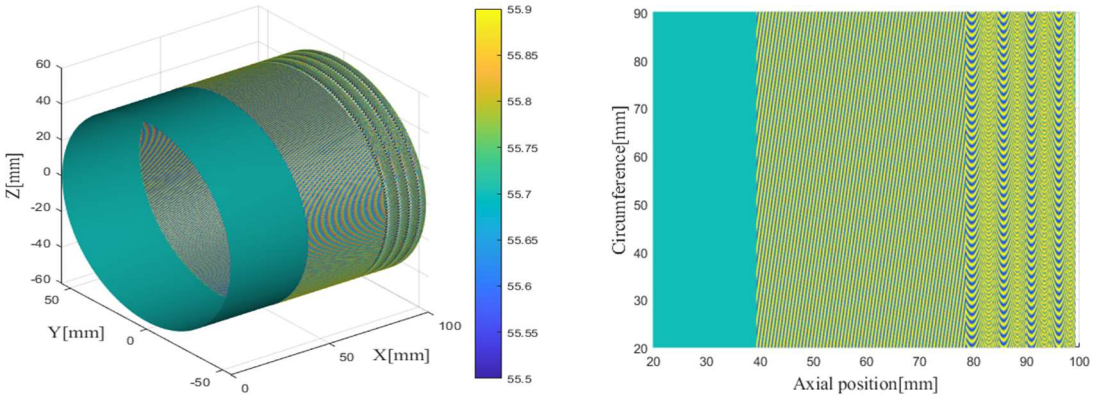

(A) (B)

Fig. 13 Reconstructed surface topographies of Tube A with signal features. (A) 3D topography; (B) 2D topography.

Moreover, what mechanism caused the chatter frequency shift during the cutting process? Recalling the mode of vibration of the thin-wall cylinder in theory (see Fig. 5) and the experimental modal analysis result (see Fig.7), we see that the two chatter frequencies were respectively close to the natural frequencies corresponding to the mode (1,1) and mode (1,3) of the machined cylinder and showed analogous change trends along the cutting path. According to Tlusty's law of machining dynamics [30,31], it is known that the chatter stability characterized by the limiting depth of cut, is dependent on the minimum of the real part of the receptance FRF of the vibrational structure, that is $d_{\lim} = -\frac{1}{2K_c \operatorname{Re}\{G(\omega)\}_{\min}}$, where K_c is the cutting coefficient and $G(\omega)$ is the receptance. Fig. 14 presents the real parts of the receptance FRFs at different tool-workpiece contact points along the axis of Tube A, where the receptance was obtained

indirectly using the relationship as $Receptance = Accelerance/(-\omega^2)$. It is seen that the stability limit of the machining process became decreased as the cutting tool moved toward the free end of the workpiece, which explains why the machining was stable at the beginning and then deteriorated progressively in the machining experiments. In addition, at the cutting points near the chuck, the minimum of the real part of the receptance (green circles) located around the mode (1,1) of the machined tube, whereas the minimum shifted and located around the mode (1,3) as the cutting point kept getting close to the free end. This indicates that the weakest mode leading to machining chatter was position-dependent on the workpiece. As a result, the distinctive patterns shown in the chatter zones 1 and 2 were mainly attributed to the contribution of the axial beam mode (1,1) and the circumferential shell mode (1,3), respectively.

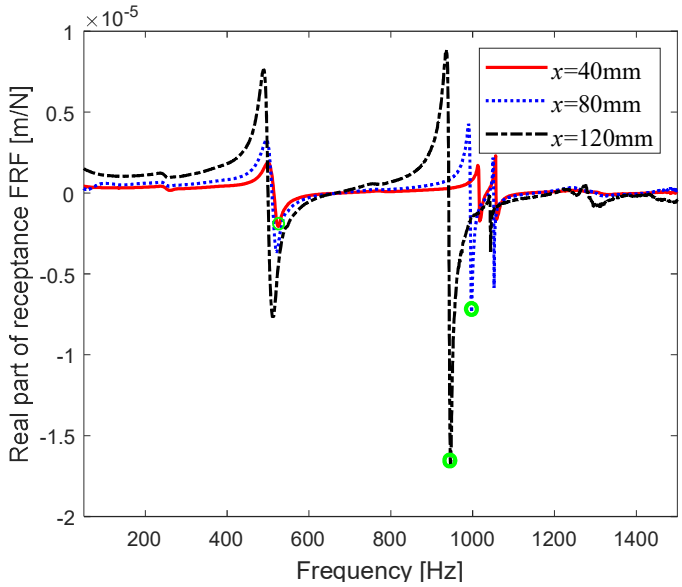

Fig. 14 Real parts of the receptance FRFs of Tube A at different cutting positions

Relative to Tube A the decreased length and increased diameter of the workpiece could make the shell mode constantly dominate in the chatter vibrations under the same machining parameters. In terms of Tube B machining test, the chatter mode shift also occurred but the duration of the beam mode-dominated chatter vibration was evidently shortened, as demonstrated in Fig. 15.

(a)

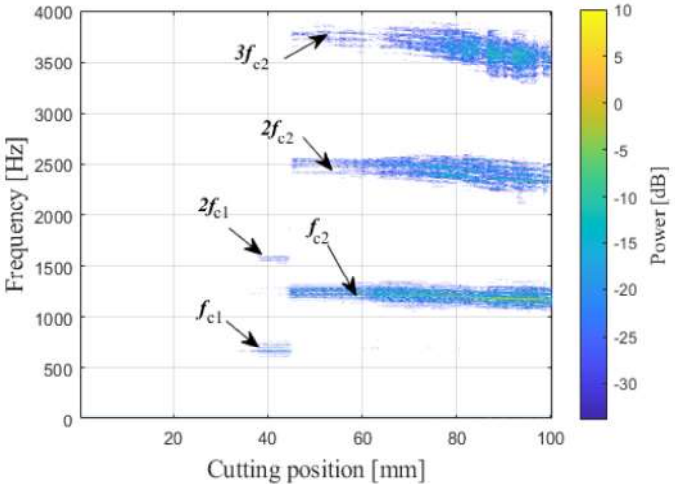

(b)

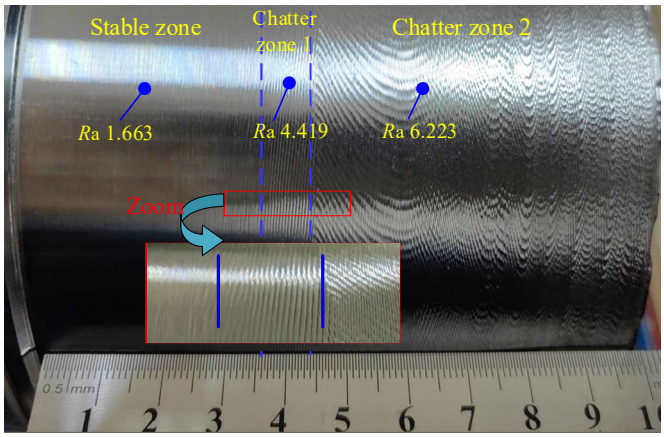

(c)

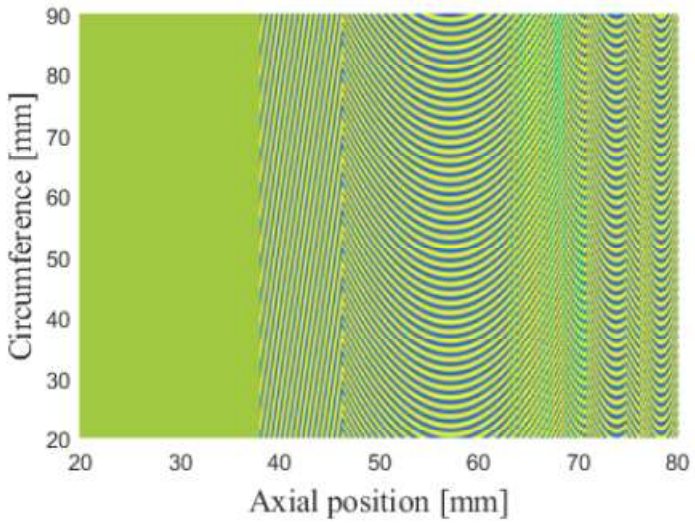

Fig. 15 Signal processing and surface topography of Tube B: (a) vibration spectrum; (b) machined surface topography; (c) reconstructed surface topography.

For machining of Tube C, as shown in Fig. 16, only the lobe-shaped patterns were found left on the finished surface, which is similar with the experimental observations reported in the studies [15,19,23,24]. By comparison, the spectrum of the vibration of

Tube C also shows a gradually decreased chatter frequency as that of the other two tubes at the chatter zone 2. It can be verified that the chatter frequency is associated with the vibration mode (1,4) of the tube. This further verifies that the circumferential shell mode of the thin-walled cylinders was more sensitive to the thickness change due to the material removal in cutting than the axial beam mode of the thin-walled cylinder.

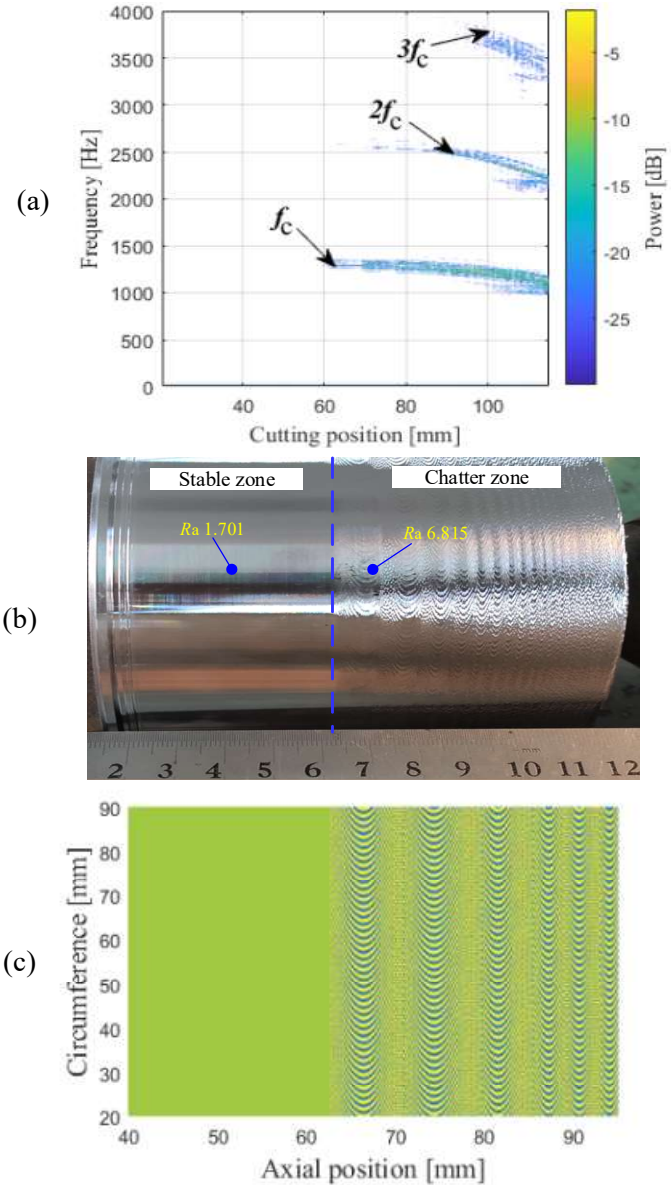

Fig. 16 Signal processing and surface topography of Tube C: (a) vibration spectrum; (b) machined surface topography; (c) reconstructed surface topography.

5. Conclusions

This paper investigates the dynamic behavior and surface quality of the clamped-free

thin-walled tubular workpieces in turning operations based on dynamics and kinematics of machining. The effects of wall thicknesses and cutting points on vibration characteristics of the machined workpiece are analyzed. Machining trials of thin-walled tubes were also conducted to explore the features of the vibration response and surface topography. According to the theoretical and experimental results, main conclusions are drawn as follows:

(1) The thin wall cylindrical workpiece vibrates in combination of the axial beam mode and the circumferential shell mode. The shell mode is more sensitive to the variation of the wall thickness of the tube during machining. As the thickness decreases, the shell mode becomes easier to be excited.

(2) The contribution of each vibrational mode of the cylinder to the response varies along the cutting path. When it is close to the chuck end, the dominant mode could be the beam mode; when it is near the free end, the vibration could be dominated by the shell mode. Also, the stability limits of the machining process decreased as the cutting tool moved toward the free end of the workpiece.

(3) During the machining process of the thin-walled cylinder machining it has been found that the chatter frequency as well as the surface textures could shift due to the change of the weakest mode of vibration leading to chatter. By using the extracted time-varying vibration frequency and roughness measurement along the cutting path, the data-driven surface topography was reconstructed, which showed consistency with the physical surface. The formulated correlation between the vibration characteristics and the surface topography provides a new insight into the dynamic behaviors of the thin-walled cylindrical workpiece machining.

Acknowledgments

The financial support of National Natural Science Foundation of China (Grant Nos. 52175108, 51805352), CACSUK Research Collaboration Seed Fund and the Royal Society (IEC\NSFC\223079) are gratefully acknowledged.

References

[1] Y. Zhang, H. Song, X. Yu, J. Yang, Modeling and analysis of forced vibration of the thin-walled cylindrical shell with arbitrary multi-ring hard coating under elastic constraint, Thin-Walled Struct. 173 (2022) 109037

[2] J. Munoa, X. Beudaer, Z. Dombovari, Y. Altintas, E. Budak, C. Brecher, G. Stepan, Chatter suppression techniques in metal cutting, CIRP Ann-Manuf Techn. 65 (2016) 785-808, https://doi.org/10.1016/j.cirp.2016.06.004.

[3] L. Croppi, N. Grossi, A. Scippa, G. Campatelli, Fixture optimization in turning thin-wall components, Machines.7 (4) (2019) 68, https://doi.org/10.3390/machines7040068.

[4] G. Wu, G. Li, W. Pan, I. Raja, X. Wang, S. Ding, A state-of-art review on chatter and geometric errors in thin-wall machining processes, J. Manuf. Processes. 68 (2021) 454-480, https://doi.org/10.1016/j.jmapro.2021.05.055.

[5] X.M. Zhang, G.R. Liu, K.Y Lam, Vibration analysis of thin cylindrical shells using wave propagation approach, J. Sound Vib. 239 (2001) 397-403, https://doi.org/10.1006/jsvi.2000.3139.

[6] X. Li, Study on free vibration analysis of circular cylindrical shells using wave propagation, J. Sound Vib. 311 (2008) 667-682, https://doi.org/10.1016/j.jsv.2007.09.023.

[7] A. Tawat, V. Matsagar, A.K. Nagpal, Finite element analysis of thin circular cylindrical shells, Proc. Indian Natl. Sci. Acad, 82(2) (2016)349–355, https://doi.org/10.16943/ptinsa/2016/48426.

[8] H. Li, K.Y. Lam, Frequency characteristics of a thin rotating cylindrical shell using the generalized differential quadrature method, Int. J. Mech. Sci. 40 (5) (1998) 443-459, https: //doi.org/10.1016/S0020-7403(97)00057-X.

[9] S. Sun, S. Chu, D. Cao, Vibration characteristics of thin rotating cylindrical shells with various boundary conditions, J. Sound Vib. 331 (2012) 4170–4186, https://doi.org/10.1016/j. jsv.2012.04.018.

[10] Sh. Hosseini-Hashemi, M.R. Ilkhani, M. Fadaee, Accurate natural frequencies and critical speeds of a rotating functionally graded moderately thick cylindrical shell, Int. J. Mech. Sci. 76 (2013) 9-20, https://doi.org/10.1016/j.ijmecsci.2013.08.005.

[11] Z. Qin, Z. Yang, J. Zu, F. Chu, Free vibration analysis of rotating cylindrical shells coupled with moderately thick annular plates, Int. J. Mech. Sci. (142-143) (2018) 127-139, https://doi.org/10.1016/j.ijmecsci.2018.04.044

[12] Y. Altintas, M. Weck, Chatter stability of metal cutting and grinding, CIRP Ann-Manuf Technol. 53 (2) (2004) 619-642, https://doi.org/10.1016/S0007-8506(07)60032-8.

[13] M. Siddhpura, R. Paurobally, A review of chatter vibration research in turning, Int. J. Mach. Tools. Manuf. 61 (2012) 27-47, https://doi.org/10.1016/j.ijmachtools.2012.05.007

[14] G. Urbikain, D. Olvera, L.N. Lopez de Lacalle, A. Beranoagirre, A. Elias-Zuniga, Prediction methods and experimental techniques for chatter avoidance in turning systems: a review, Appl. Sci.-Basel. 9 (2019) 4718, https://doi.org/10.3390/app9214718.

[15] R.N. Arnold, Chatter patterns formed on the surface of thin cylindrical tubes during machining, J. Mech. Eng. Sci. 3 (1) (1961) 7–14, https://doi.org/10.1243/JMES_JOUR_1961_003_004_02.

[16] J. Y. Chang, G. J. Lay, M. F. Chen, A study of the chatter characteristics of the thin wall cylindrical workpiece, in: Int. J. Mach. Tools Manuf, 1994, pp. 489–498.

[17] G.J. Lai, J.Y. Chang, Stability analysis of chatter vibration for a thin-wall cylindrical workpiece, Int.

J. Mach. Tools Manuf. 35 (3) (1995) 434-444, https://doi.org/10.1016/0890-6955(94)E0011-7.

[18] K. Mehdi, J.F. Rigal, D. Play, Dynamic behavior of a thin-walled cylindrical workpiece during the turning process, Part 1: Cutting process simulation, J. Manuf. Sci. Eng. 124 (3) (2002) 562–568, https://doi.org/10.1115/1.1431260.

[19] K. Mehdi, J.F. Rigal, D. Play, Dynamic behavior of a thin-walled cylindrical workpiece during the turning process, Part 2: Experimental approach and validation, J. Manuf. Sci. Eng. 124 (3) (2002) 569–580, https://doi.org/10.1115/1.1432667.

[20] Z. Sahraoui, K. Mehdi, M. Ben-Jaber, Analytical and experimental stability analysis of AU4G1 thin-walled tubular workpieces in turning process, Proc. Inst. Mech. Eng., Part B: J. Eng. Manuf. 234 (6-7) (2020) 1007-1018, https://doi.org/10.1177%2F0954405419896115.

[21] P. Lorong, A. Larue, A. P. Duarte, Dynamic study of thin wall part turning, Adv. Mater. Res. 223 (2011) 591–599, https://doi.org/10.4028/www.scientific.net/AMR.223.591.

[22] A. Fischer, P. Eberhard, Parametric flexible multibody model for material removal during turning, J. Comput. Nonlin. Dyn. 9 (1) (2014) 011007, https://doi.org/10.1115/1.4025283.

[23] A. Gerasimenko, M. Guskov, P. Lorong, J. Duchemin, A. Guskov, Experimental Investigation of Chatter Dynamics in Thin-walled Tubular Parts Turning. Paper presented at the Proceedings of the Thirteenth International Conference on High Speed Machining, France, 2016.

[24] A. Gerasimenko, M. Guskov, A. Guskov, P. Lorong, et al., Analytical modeling of a thin-walled cylindrical workpiece during the turning process. Stability analysis of a cutting process, J. Vibroeng. 19 (8) (2017) 5825-5841, https://doi.org/10.21595/jve.2017.18061.

[25] C.X. Wang, X.W. Zhang, X.F. Chen, H.R. Cao, Time-varying chatter frequency characteristics in thin-Walled workpiece milling with B-Spline wavelet on interval finite element method, Journal of Manufacturing Science and Engineering 141 (2019), 051008

[26] J.N. Reddy, Theory and Analysis of Elastic Plates and Shells, 2nd Edition, CRC, 2007.

[27] G. Tosello, G. Bissacco, J. Cao, D. Axinte, Modeling and simulation of surface generation in manufacturing, CIRP Ann-Manuf Technol. (2023), https://doi.org/10.1016/j.cirp.2023.05.002

[28] G. Stepan, A.K. Kiss, B. Ghalamchi, J. Sopanen, D. Bachrathy, Chatter avoidance in cutting highly flexible workpieces, CIRP Ann-Manuf Technol. 66 (2017) 377–380, https://doi.org/10.1016/j.cirp.2017.04.054.

[29] K. Lu, Y. Wang, F. Gu, X. Pang, A. Ball, Dynamic modeling and chatter analysis of a spindle-workpiece-tailstock system for the turning of flexible parts, Int. J. Adv. Manuf. Technol. 104 (2019) 3007–3015, https://doi.org/10.1007/s00170-019-04224-w.

[30] Y. Altintas, Manufacturing automation: metal cutting mechanics, machine tool vibrations, and CNC design, Cambridge, 2012.

[31] K. Lu, F. Gu, A. Longstaff, G. Li, An investigation into tool dynamics adaptation for chatter stability enhancement in the turning of flexible workpieces, Int. J. Adv. Manuf. Technol. 111 (2020) 3259–3271, https://doi.org/10.1007/s00170-020-06339-x.